

# Optimizing Prediction Serving on Low-Latency Serverless Dataflow

Vikram Sreekanti  
UC Berkeley

Harikaran Subbaraj  
UC Berkeley

Chenggang Wu  
UC Berkeley

Joseph E. Gonzalez  
UC Berkeley

Joseph M. Hellerstein  
UC Berkeley

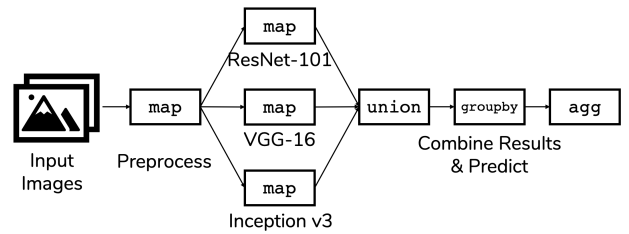
## Abstract

*Prediction serving* systems are designed to provide large volumes of low-latency inferences from machine learning models. These systems mix data processing and computationally intensive model inference, and benefit from multiple heterogeneous processors and distributed computing resources. In this paper, we argue that a familiar dataflow API is well-suited to this latency-sensitive task, and amenable to optimization even with unmodified black-box ML models. We present the design of *Cloudflow*, a system that provides such an API and realizes it on an autoscaling serverless back-end. Cloudflow transparently implements performance-critical optimizations including operator fusion and competitive execution. Our evaluation shows that Cloudflow’s optimizations yield significant performance improvements on synthetic workloads and that Cloudflow outperforms state-of-the-art prediction serving systems by as much as  $2\times$  on real-world prediction pipelines, meeting latency goals of demanding applications like real-time video analysis.

## 1 Introduction

Machine learning has become ubiquitous over the last decade in an increasingly broad set of fields, ranging from manufacturing to medicine and sports. Much of the systems research surrounding machine learning has focused on improving the infrastructure that supports the creation of models—tools like Tensorflow [1], PyTorch [46], and MLLib [42] have greatly simplified the process of developing and training models at scale. The models trained in these systems are deployed in numerous applications—generating social media feeds, enabling chat bots, designing video games, and so on.

This process of deploying a trained model for use in a larger application is often called *prediction serving*. Prediction serving is a particularly interesting task because it combines the complex computations of machine learning with the performance requirements of interactive applications. More specifically, it has three key properties: (1) it is *computationally*



```

1  fl = cloudflow.Dataflow(['url', str])
2  img = fl.map(img_preproc)
3  p1 = img.map(resnet_101)
4  p2 = img.map(vgg_16)
5  p3 = img.map(inception_v3)
6  fl.output = p1.union(p2,p3).groupby(rowID).agg(max, 'conf')

```

Figure 1: An example prediction serving pipeline to classify a set of images using an ensemble of three models, and the Cloudflow code to specify it. The models are run in parallel; when all finish, the result with the highest confidence is output.

*intensive*; (2) it is a part of an interactive application, meaning it has *low latency requirements*; and (3) it is *compositional*, meaning a single request passes through multiple stages. Figure 1 shows an example prediction serving pipeline, which normalizes an input image, runs three image classification models in parallel, and combines the results to make a prediction (often called a *model ensemble*).

Commercial services like AWS Sagemaker and Azure ML have emerged in recent years to attempt to fill this gap. These systems deploy individual models as separate microservices which enables neat modularity of pipeline stages. However, this approach gives the system no visibility into the *structure* of the computation and how the individual microservices relate to each other, which significantly complicates debugging and limits end-to-end performance optimization.

Alternately, Pretzel [37] is a recent research system which explored fine-grained optimizations of *white-box*, dataflow-style prediction pipelines that leverage full visibility into the pipeline and the semantics of each stage. However, this approach also requires the developer to rewrite their *individual*

*models* (i.e., pipeline stages) in Pretzel’s DSL, which is cumbersome and limits model development. It also makes Pretzel inflexible to innovations in machine learning frameworks.

In this paper, we argue for a natural middle ground: a simple dataflow API for prediction pipelines based on arbitrary (black-box) operators, which are typically models trained by users in their library of choice (e.g., TensorFlow, PyTorch, Scikit-Learn). Rather than requiring models to be rewritten in a white-box fashion, a graph of familiar dataflow operators (e.g., `map`, `filter`, `join`) can be used to wrap black-box models. The dataflow API also provides visibility into the structure of the pipeline, which allows for the end-to-end computation to be optimized—e.g., two operators that have large data dependencies might be fused together.

Existing large-scale distributed dataflow systems are not well suited for prediction serving for two reasons. First, prediction serving tasks have low latency requirements. Systems like Apache Spark [60] and Apache Flink [8], however, are optimized for throughput rather than for minimizing tail-latency.

Second, prediction serving systems—like all interactive applications—must operate in the presence of bursty and unpredictable workloads [21, 50], which requires fine-grained resource allocation. Unfortunately, efforts [14, 15, 32, 33, 38, 39] to address operator-level auto-scaling have primarily focused on meeting throughput requirements.

We present Cloudflow, a dataflow system for prediction serving pipelines. Cloudflow is built on top of Cloudburst [52], a stateful serverless programming platform. Cloudburst is a Functions-as-a-Service (FaaS) system that provides low-latency access to state by enabling function composition, message passing, and caching of frequently accessed data. Layering on top of a stateful serverless platform enables fine-grained resource allocation, provides a simple functional programming model to match dataflow, and supports efficient state retrieval.

Cloudflow exposes a dataflow API that enables simple composition patterns common in prediction serving. The dataflow model enables us to apply both dataflow and prediction serving optimizations (e.g., operator fusion, competitive execution) to optimize those pipelines, even while treating models as black boxes. We demonstrate that these optimizations can be applied without user intervention. In practice, Cloudflow is able to outperform prior systems for prediction serving by as much as  $2\times$ , and—critically—meets latency goals of demanding applications like real-time video analysis.

In sum, the contributions of this paper are as follows:

- The modeling and implementation of prediction serving pipelines as dataflow graphs using a familiar API of functional operators. This includes the implementation of common patterns like ensembles and cascades.
- Leveraging and extending a stateful serverless platform to enable efficient dataflows without changes to user programs, as discussed in Sections 3 and 4.

- The automatic application of well-studied optimizations from the dataflow and prediction serving domains to Cloudflow dataflows.
- A thorough evaluation of Cloudflow, demonstrating the benefits of optimized dataflow on both synthetic benchmarks and on real-world prediction pipelines.

## 2 Background and Motivation

In this section, we discuss challenges posed by prediction serving (Section 2.1). We then argue that dataflow is well-suited to address these challenges and discuss how we optimize prediction pipelines (Section 2.2), and we motivate the use of a serverless runtime and our choice, Cloudburst (Section 2.3).

### 2.1 Prediction Serving

Prediction serving has become a common part of many tasks, such as organizing social media news feeds, responding to voice assistant queries (Alexa, Siri, etc.), detecting fraud in financial transactions, and analyzing radiological scans. The models used in these applications, particularly with the advent of deep neural networks, can be incredibly computationally intensive [20, 28]. As a result, it has become commonplace for these models to run on specialized hardware, like GPUs or Google’s TPU (Tensor Processing Unit) [31].

Furthermore, these applications are often interactive and require predictions to be made within tight latency bounds. Facebook published a detailed case study [21] in which they describe models that query user-specific state and generate predictions in real-time—about a few hundred milliseconds. Predictions that miss their latency deadlines are usually discarded in favor of a default response [23, 63], making it critical to minimize both median *and* tail (99th percentile) latencies.

Importantly, it is typical for applications to compose multiple models to make a single prediction [37]. Consider the example in Figure 1. This image classification pipeline first preprocesses and normalizes an image, and then runs three different models in parallel—each has different specializations. The results of all three models are aggregated to generate a prediction. This particular pattern is called a *model ensemble*.

### 2.2 Dataflow and Optimizations

The sequence of tasks in a prediction pipeline forms a natural dataflow graph: Each stage of the pipeline receives an input, applies a transformation, and passes the result downstream. The output of the last stage is the prediction rendered by the whole pipeline. Using a traditional dataflow model with operators like `map`, `filter`, and `join` makes constructing pipelines easy—the ensemble in Figure 1 being a case in point. On inspection this may seem straightforward, but it is in stark contrast with existing systems: AWS Sagemaker

forces users to manually construct containers for each model stage, while Pretzel [37] requires users to rewrite their models in a custom API to leverage the system’s optimizations. In this paper, we argue that a traditional dataflow API enables us to implement a number of pipeline optimizations *without* requiring any modification of black-box ML models.

We focus on five optimizations from the data processing and prediction serving literature that apply here [3, 7, 10, 27, 36, 37], but this list is not meant to be exhaustive.

**Operator Fusion.** Separate stages in a dataflow may pass significant data like videos or images. To minimize communication, it can be beneficial to fuse these operators to avoid data movement.

**Competitive Execution.** Machine learning models can have highly variable execution times [35], depending on model structure and input complexity. Similar to straggler mitigation in MapReduce [11], competitive execution of inference has been shown to improve tail latencies for ML models [36, 53].

**Operator Autoscaling and Placement.** Given the diversity of compute requirements in a pipeline (e.g., simple relational operations vs neural-net inference), we often want to devote more—and more specialized—resources to bottleneck tasks.

**Data Locality.** While prediction pipelines are typically computationally intensive tasks, they also often involve significant data access [19]. Remote data access can easily become a bottleneck unless we optimize for data locality by placing computations near cached data.

**Batching.** Large models like neural nets can benefit greatly from batched execution on vectorized processors like GPUs [5, 16], resulting in better throughput at the cost of higher latency. The improved throughput translates into better resource utilization and thereby reduces costs.

In Section 4 we explore each of these optimizations in more detail, and explain how we deliver on them in Cloudflow.

## 2.3 Deploying Prediction Pipelines

Having motivated the use of dataflow to construct and optimize prediction pipelines, we now consider the runtime on which they are executed. Two key concerns affect our decision: (1) tight latency constraints, and (2) nimble responses to unpredictable workload changes. Unfortunately, batch streaming dataflow systems (e.g., Apache Flink [8], Apache Spark [60]) are unsuitable on both counts—they are throughput-oriented systems that do not scale easily.

Instead, we chose to use serverless Functions-as-a-Service (FaaS) infrastructure, primarily because FaaS systems natively support fine-grained elasticity—an integral part of operator autoscaling. Additionally, FaaS’ functional programming style neatly matches the operator-based abstractions of dataflow—each operator can be deployed as a separate function.

Despite the benefits of fine-grained elasticity, commercial FaaS offerings have key shortcomings around data in-

tensive workloads [24]—they have high invocation latencies and force users into data-shipping antipatterns. To overcome these limitations, we turned to research platforms like Archipelago [51], OpenLambda [25], and Cloudburst [52] as more performant alternatives. Of these, we chose Cloudburst as Cloudflow’s underlying compute engine because—in addition to standard FaaS autoscaling—it enables low-latency function composition and data access. We provide a brief overview of the system here and refer the interested reader to [52].

Cloudburst is a FaaS platform that supports stateful serverless programming with three kinds of state sharing: function composition, message passing, and data lookups in caches located on the same machines where code is run. The system is built on top of Anna [58, 59], a low-latency autoscaling key-value store. Cloudburst layers a set of function executor nodes on top of Anna; each executor has multiple workers that respond to user requests as well as a cache that intermediates on KVS reads and writes. The system optimizes for data locality by scheduling requests on executor nodes where input data is likely to be cached. Cloudburst is able to outperform commercial FaaS platforms by orders of magnitude for stateful tasks and significantly cut data transfer costs.

In addition to the standard FaaS execution model, Cloudburst allows users to pre-register compositions of functions as directed acyclic graphs (DAGs); a whole DAG is scheduled and executed with a single user request. Combined with the stateful architecture, this DAG-based programming model is a natural fit for deploying prediction dataflows. While Cloudburst was a good starting point for our infrastructure, the system nonetheless had a number of key limitations that we had to overcome—we describe these in Section 4.

## 3 Architecture and API

In this section, we describe the Cloudflow API for composing dataflows, how that API captures common prediction pipelines, and how Cloudflow pipelines are compiled down to Cloudburst serverless functions.

### 3.1 Dataflow API

The Cloudflow API centers around three main concepts: a simple `Table` type for data, computational `Operators` that compute over `Tables`, and a functional-style `Dataflow` to author specifications of DAGs of `Operators`. A Python program can specify a `Dataflow` and execute it on a `Table`; the Cloudflow runtime is responsible for taking that specification and invoking the `Operators` to generate an output `Table`.

The core data structure in Cloudflow is a simple in-memory relational `Table`. A `Table` has a *schema*, which is a list of column descriptors, each consisting of a name and an associated data type (e.g., `str`, `int`). It also has an optional *grouping col-*

API	Inputs	Output Type	Description
map	fn: $(c_1, \dots, c_n) \rightarrow (d_1, \dots, d_m)$ , table: $\text{Table}[c_1, \dots, c_n][\text{column?}]$	$\text{Table}[d_1, \dots, d_m][\text{column?}]$	Apply a function <code>fn</code> to each row in <code>table</code>
filter	fn: $(c_1, \dots, c_n) \rightarrow \text{bool}$ , table: $\text{Table}[c_1, \dots, c_n][\text{column?}]$	$\text{Table}[c_1, \dots, c_n][\text{column?}]$	Apply Boolean function to each row in <code>table</code> and include only rows with true results
groupby	column: str, table: $\text{Table}[c_1, \dots, c_n][\text{column?}]$	$\text{Table}[c_1, \dots, c_n][\text{column?}]$	Group rows in an ungrouped <code>table</code> by the value in <code>column</code>
agg	agg_fn: $\{c_i\} \rightarrow d$ , table: $\text{Table}[c_1, \dots, c_n][\text{column?}]$	$\text{Table}[\text{column?}, d][\text{column?}]$	Apply a predefined aggregate function <code>agg_fn</code> (count, sum, min, max, avg) to column $c_i$ of <code>table</code>
lookup	key: str? $c_k?$ , table: $\text{Table}[c_1, \dots, c_n][\text{column?}]$	$\text{Table}[c_1, \dots, c_n, \text{key}][\text{column?}]$	Retrieve an object from the underlying KVS and insert into the <code>table</code>
join	left: $\text{Table}[c_1, \dots, c_n][\text{column?}]$ , right: $\text{Table}[d_1, \dots, d_m][\text{column?}]$ , key: str? how: left?, outer?	$\text{Table}[c_1, \dots, c_n, d_1, \dots, d_m][\text{column?}]$	Join two Tables on key, using the automatically assigned query ID as a default. Optionally specify left join or (full) outer join mode.
union	$\{\text{Table}[c_1, \dots, c_n][\text{column?}], \dots\}$	$\text{Table}[c_1, \dots, c_n][\text{column?}]$	Form union of many Tables with matching schemas.
anyof	$\{\text{Table}[c_1, \dots, c_n][\text{column?}], \dots\}$	$\text{Table}[c_1, \dots, c_n][\text{column?}]$	Pick any one of many Tables with matching schemas.
fuse	sub_dag: Flow, table: $\text{Table}[c_1, \dots, c_n][\text{column?}]$	$\text{Table}[d_1, \dots, d_m][\text{column?}]$	An encapsulated chain of operators (see Section 4)

Table 1: The core Operators supported by Cloudfow. Each accepts a Table as input and returns a Table as output. Our table type notation here is  $\text{Table}[c_1, \dots, c_n][\text{column}]$ , where  $c_1, \dots, c_n$  is the schema, and `column` is the grouping column. Optional items are labeled with a `?`.

```

1 fl = cloudfow.Dataflow(['jpg_url', str])
2 img = fl.map(img_preproc)
3 pred = img.map(resnet)
4 label = pred.map(convert_to_label)
5 fl.output = label
6 fl.deploy()
7
8 input_tbl = \
9     Table(['jpg_url', str], \
10          ['s3://mybucket/cats.jpg', 's3://mybucket/dogs.jpg'])
11 out = fl.execute(input_tbl)
12 out.result()

```

Figure 2: A script to create a Cloudfow dataflow and execute it once.

`umn`<sup>1</sup>. We briefly defer our description of grouping columns to the discussion below of the dataflow operators in Table 1.

A Cloudfow `Dataflow` represents a *specification* for a DAG of dataflow operators with a distinguished input and output, as in Figure 1. One can think of a `Dataflow` as a declarative query, or a lazy functional expression, describing how to compute an output table from an input table. We step through Figure 2 to illustrate. A `Dataflow` instance is instantiated with an input schema (Figure 2, line 1). To construct pipelines, the `Dataflow` class includes a set of method names that correspond one-to-one with the `Operator` names in Table 1; these methods generate new `Dataflow` objects that append the specification of the corresponding operator onto their input dataflow. So, for example line 2 represents a dataflow that has a single-column table as its input, followed by the expression `map(img_preproc)`; line 3 represents a dataflow equivalent to `flow.map(img_preproc).map(resnet)`, and so on. `Dataflow fl` is *valid* after its output member is as-

<sup>1</sup> Our syntax naturally extends to support a list of grouping columns, but we omit that detail here for descriptive simplicity. Even without that syntax, one can form composite grouping columns with a `map` operator.

signed (line 5). This assignment requires its right-hand-side to be derived from the same `Dataflow fl`, representing a connected flow from the input to the output of `fl`.

To prepare a `Dataflow` for execution, we use the `deploy` method (line 6), which compiles the `Dataflow` and registers it with the Cloudburst runtime. Once deployed, we can repeatedly execute the `Dataflow` by passing in a `Table` with the corresponding schema. `execute` immediately returns a Python future that represents the result table of the execution (line 11). Cloudburst schedules and executes the DAG as described in [52], and results are stored in Anna. The result is accessed by calling the `result` method of the future returned by `execute` (line 12). During execution of a `Dataflow`, each row in the input is automatically assigned a unique row ID, which stays with the row throughout execution.

**Dataflow Operators.** The set of Cloudfow Operators is similar to the relational algebra, or the core of a dataframe API. It consists of a small set of dataflow operators, each of which takes in `Tables` and produces a `Table`. Table 1 provides an overview of the input/output types of each operator. The operators look familiar from batch processing and dataframe libraries, but recall that our focus here is on lightweight, interactive predictions over small in-memory request `Tables`.

The `map`, `filter`, `join` and `union` operators are fairly standard. `groupby` takes an ungrouped `Table` and returns a grouped `Table`. `map`, `filter`, `union`, `anyof` and `fuse` all accept `Tables` that can be grouped or ungrouped (denoted by `[column?]`) and return `Tables` with the same grouping. `anyof` passes exactly one of its input tables to the output; the decision is left up to the runtime (Section 4). `fuse` is an internal operator that executes multiple other operators over a `Table`—we discuss its use in Section 4.

The `agg` operator supports basic aggregations: counts, sums, averages, min, and max. When `agg` is applied over an ungrouped table, it returns a table with a single row; when applied over a grouped table, `agg` returns an ungrouped table with one row per input group containing the group value and aggregate result. `join` takes two input tables, both of which must be ungrouped, and joins them on a user-specified key; if no key is specified, the two tables are joined on the row ID. Cloudflow also supports left joins, where rows from the left table are included in the output even if there is no match in the other table, and outer joins, in which rows from each table are included in the output even if there are no matches.

Finally, `lookup` allows dataflows to interact with data outside the input table. Specifically it allows for reads from the Anna KVS that Cloudburst uses for storage. `lookups` can take either a constant or a column reference. If the input is a column reference  $c_k$ , the effect is akin to a join with the KVS: for each input row, Cloudflow retrieves the matching object in the KVS. As we discuss in Section 4, we use the information in the `lookup` operator to take advantage of Cloudburst’s locality-aware scheduling. In practice, many of the API calls in Table 1 have other arguments for user convenience (e.g., naming output columns) and to give Cloudflow hints about resource requirements and optimizations (e.g., requires a GPU, supports batching). We omit describing these for brevity.

**Typechecking and Constraints.** Similar to TFX [4], Cloudflow supports basic typechecking to ensure the correctness of pipelines. If the input type of an operator does not match the output type of the previous operator, Cloudflow raises an error.

To this end, we require programmers to provide Python type annotations for the functions they pass into `map` and `filter`. Since Python is a weakly-typed language, these type annotations do not guarantee that the data returned by a function matches the annotation. At runtime, the type of each function’s output is inspected using Python’s `type` operator. Once again, if the type does not match the function’s annotation, Cloudflow raises an error. This prevents Python from arbitrarily coercing types, causing pipelines to fail silently—generating incorrect or nonsensical results without surfacing an error.

### 3.2 Prediction Serving Control Flow

Having described Cloudflow’s dataflow model, we show how it simplifies the implementation of control flow constructs common in prediction pipelines. We describe some patterns and highlight their simplicity with code snippets. This section is not meant to be exhaustive—rather we illustrate Cloudflow’s fitness for standard prediction serving control flow.

**Ensembles.** In an ensemble pattern (e.g., Figure 1), an input is evaluated by multiple models in parallel. After all models finish evaluating, the results are combined, either by picking the

```

1 flow = cloudflow.Dataflow(['jpg_url', str])
2 img = flow.map(preproc)
3 simple = img.map(simple_model)
4 complex = simple.filter(low_confidence).map(complex_model)
5
6 flow.output = simple.join(complex, how='left').map(max_conf)

```

Figure 3: A simple two-model cascade specified in Cloudflow.

prediction with the highest confidence or by taking a weighted vote of the results. Figure 1 shows a Cloudflow implementation of a model ensemble. After a preprocessing stage (line 2), three models are evaluated in parallel (lines 3-5), the results are unioned, and a final prediction is selected by using `agg` to pick the prediction with the maximum confidence (line 6).

**Cascades.** In a cascade, models of increasing complexity are executed in sequence. If an earlier model returns a prediction of sufficiently high confidence, then later models are skipped. Figure 3 shows the Cloudflow implementation of a model cascade. After the simple model is executed (line 3), we retain rows with low confidence and apply the complex model to them (line 4). We then join the simple and complex models’ results using a left join to include rows that were filtered out from the simple model (line 6). We then apply a `max_conf` function to report the prediction with the highest confidence.

### 3.3 Discussion

In addition to the dataflow operators highlighted in Table 1, Cloudflow also has an `extend` method. `extend` takes in another valid flow as an argument and appends its DAG to the existing flow, creating a dataflow that chains the pair. This allows for the easy composition of two flows. For example, multiple users in an organization might share an image preprocessing flow to which they each append a custom image classification flow.

In sum, Cloudflow’s API significantly simplifies the process of constructing prediction pipelines as compared to other systems. Our dataflow model provides natural abstractions for *composition*—e.g., chains of user-defined code in Figure 2, parallel executions with joins in Figures 1 and Figure 3. AWS Sagemaker has limited support for prediction pipelines—all operators must be in a sequence—and AzureML and Clippier have no support for multi-stage pipelines to our knowledge.

Additionally, Cloudflow takes simple Python specs and automatically deploys pipelines for the user in a serverless framework. AzureML and Sagemaker require users to create custom containers for each stage<sup>2</sup>. As we discuss in Section 5.2.2, porting pipelines to other systems required writing and deploying long-lived driver programs to manage each request as it moved through a pipeline—something we avoid altogether in Cloudflow.

<sup>2</sup>These systems will automatically generate a containerized version of the model only if you use their development infrastructure end-to-end.

Finally, using a dataflow abstraction makes the resulting DAG of computation amenable to a variety of optimizations. We turn to that topic next.

## 4 Optimizing Dataflows

In this section, we describe the Cloudflow implementation of each of the optimizations from Section 2.2. All the techniques described in this section are automatic optimizations; the user only needs to select *which* optimizations to enable. We return to the topic of automating optimization selection in Section 7. Automatic optimization is a key benefit of the dataflow model, allowing users to focus on pipeline logic, while Cloudflow takes care of operational concerns including deployment and scheduling.

The Cloudflow dataflow API produces a DAG of operators selected from Table 1. Cloudburst provides a lower-level DAG-based DSL for specifying compositions of black-box Python functions [52]. A naive 1-to-1 mapping of a user’s Cloudflow DAG into an isomorphic Cloudburst DAG will produce correct results, but we show in this section that we can do much better.

Our compilation occurs at two levels. **Dataflow rewrites** captures static Cloudflow-to-Cloudflow optimizations within the dataflow topology, including operator fusion and competitive execution. **Dataflow-to-FaaS compilation** translates Cloudflow dataflows to Cloudburst DAGs that expose opportunities for dynamic runtime decisions in the FaaS infrastructure. These include *wait-for-any* DAG execution, autoscaling and hardware-aware function placement, locality-aware scheduling and batching.

In many cases Cloudburst was not designed to leverage optimizations apparent at the Cloudflow layer. As a result we had to extend Cloudburst in terms both of its API and its runtime mechanisms; we highlight these changes below.

**Operator Fusion** In operator fusion, a chain of operators within a Cloudflow DAG is encapsulated into a single `fuse` operator. The benefit of `fuse` is that it is compiled into a single Cloudburst function; as a result, the Cloudburst DAG scheduler places all logic within `fuse` at a single physical location for execution. With fusion enabled, Cloudflow will greedily fuse together all operators in a chain, but will optionally avoid fusing operators with different resource requirements (CPUs vs GPUs).

**Competitive Execution** Competitive execution is used to reduce the tail latency (usually 95th or 99th percentile) of operators with highly variable execution times. Executing multiple replicas of such operators in parallel significantly reduces perceived latency [36, 53, 56]. This is a straightforward dataflow rewrite in Cloudflow: we create redundant parallel replicas of the operator in question and add an `anyof` to consume the results. Then the runtime can choose the replica that completes first.

Cloudburst’s DAG execution API was ill-suited to `anyof`: It waits for every upstream function in the DAG before executing a function (*wait-for-all* semantics). We modified Cloudburst to enable functions to execute in *wait-for-any* mode.

**Operator Autoscaling and Placement** Each operator in a dataflow may have different performance needs—memory consumption, compute requirements and so on. This heterogeneity is particularly pronounced in AI prediction serving. For example, an image processing flow might use a CPU-intensive preprocessing stage before a GPU-based neural net.

We seek two optimizations: per-operator autoscaling decisions, and the scheduling of each operator to run on well-chosen hardware. Continuing our example, if the preprocessing stage was serialized and slow, while the neural net stage was efficient and supported batching, it makes sense to deploy preprocessing functions onto many CPU nodes, and the neural net onto fewer GPU nodes.

Cloudflow’s dataflow model makes it easy to autoscale dataflow pipelines in a fine-grained way. As described above, the Cloudflow compiler translates each operator into a separate Cloudburst function (unless fused). Like other FaaS systems, Cloudburst natively autoscales function individually: it adds and removes replicas as load (across many execution requests) changes.

However, Cloudburst—like most FaaS systems—does not support specialized hardware today. We extended Cloudburst’s runtime to add support for GPUs in addition to regular CPU-based executors. Then we extended the Cloudburst API to allow functions to be annotated with different resource class labels, and enhanced the Cloudburst scheduler to partition its task pool by label. The default Cloudburst scheduling policy is applied within each class. It is interesting to consider new policies in this context, but beyond the scope of this paper.

**Data Locality via Dynamic Dispatch** Data retrieval is an important part of many prediction pipelines. For example, a recommender system might look at a user’s recent click history, then query a database for a set of candidate products before returning a set of recommended items. Ideally, we want to avoid fetching data over the network, as this can quickly become a latency bottleneck. Cloudburst, by default, performs locality-aware scheduling—it attempts to schedule computation on machines where the task’s data dependencies are likely to be cached. However, its API requires that all of a request’s data dependencies be *pre-declared*. This conflicts with the dynamic nature of many prediction pipelines—in the example above, the candidate product set is determined by the user’s recent actions, so the Cloudburst scheduler will not know the request’s dependencies *a priori*. Avoiding this pitfall requires both Cloudflow rewrites and a Cloudburst modification.

We implement two Cloudflow rewrites. First, Cloudflow fuses each `lookup` operator with the operator downstream from it, so that the processing is colocated with the `lookup`.

Second, Cloudflow rewrites lookup operators to enable Cloudburst to perform *dynamic dispatch* of the (fused) operator at a machine that has cached the column value. To support this, the column argument to `Lookup` is converted to a reference `ref` that Cloudburst can process at runtime. The Cloudflow compiler then splits the dataflow just before the `lookup`, and generates *two* Cloudburst DAGs, flagging the first DAG with a *to-be-continued*(`d, ref`) annotation, where `d` is a pointer to the second DAG.

We then modified the Cloudburst runtime to support *to-be-continued* annotations. When a *to-be-continued* DAG finishes executing in Cloudburst, the result—rather than being returned to the user—is sent back to the Cloudburst scheduler along with a resolved `ref` (a KVS key) and the DAG ID `d`. Given the `ref`, the scheduler can place the DAG `d` on a machine where the KVS entry is likely to already be cached.

**Batching** Batching is a well-known optimization for prediction serving, taking advantage of the parallelism afforded by hardware accelerators like GPUs. Many popular ML libraries like PyTorch offer APIs that perform a batch of predictions at once. Because our dataflow model is based on small request `Tables`, we augment our runtime to form batches across invocations of `execute`. To support this, Cloudflow’s API provides a flag for the function arguments to `map` and `filter` to declare batch-awareness. We then modified the Cloudburst API to recognize that flag as we pass it down in compilation. Finally we modified the Cloudburst executor, so that when it is running a batch-enabled function, it dequeues multiple execution requests and executes the entire batch in a single invocation of the function. The maximum batch size is configurable (defaults to 10). The executor demultiplexes the results, and the API returns results for each invocation separately.

**Tradeoffs and Limitations** It is worth noting that the optimizations we discuss here have clear tradeoffs. For example, operator fusion is at odds with fine-grained autoscaling: If a slow function and a fast function are fused, an autoscaler cannot selectively allocate more resources to each function. However, automated strategies for trading off these optimizations, such as a cost-based optimizer or a planner, are out of scope for this paper. We focus on the architecture and mechanisms that enable optimized dataflows; we return to the idea of automated optimization in Section 7.

## 5 Evaluation

In this section, we present a detailed evaluation of Cloudflow. Section 5.1 studies each of the optimizations from Section 4 in isolation using synthetic workloads. We then compare Cloudflow against state-of-the-art industry and research systems on real-world pipelines. We ran all experiments on AWS in the us-east-1a availability zone. Cloudburst CPU nodes used `c5.2xlarge` instances (2 executors per machine); GPU nodes used `g4dn.xlarge` instances with Tesla T4 GPUs.

### 5.1 Optimization Microbenchmarks

We evaluate each of the proposed optimizations in isolation on synthetic workloads.

#### 5.1.1 Operator Fusion

We first study the benefits of operator fusion on linear chains of functions. The main benefit of fusion is avoiding the cost of data movement between compute locations. Correspondingly, this experiment varies two parameters: the length of the function chain and the size of data passed between functions. The functions themselves do no computation—they take an input of the given size and return it as an output. The output is passed downstream to the next function in the chain.

For each combination of chain length and size, we measure an optimized (fused) pipeline and an unoptimized pipeline. The fused pipelines execute all operators in a single Cloudburst function, while the unfused pipelines execute every stage in a separate Cloudburst function. Figure 4 reports median (bar) and 99th percentile (whisker) latencies for each setting.

As expected, for each input data size, the median latency of the optimized pipelines is roughly constant. The 99th percentile latencies have slightly more variation—generally expected of tail latencies—but there is no discernible trend. The median latencies of the unoptimized pipelines increase linearly with the length of the function chain—primarily because the cost of data movement increases with the length of the chain. For smaller chains, we see that fusion only improves latencies by 20-40%, depending on data size; however, fusing longer chains leads to improvements up to  $4\times$ .

**Takeaway:** *Operator fusion in Cloudflow yields up to a  $4\times$  latency decrease by avoiding the overheads of data serialization and data movement between function executors.*

#### 5.1.2 Competitive Execution

We proposed competitive execution to reduce latencies for operators with variable runtimes. As discussed in Section 4, Cloudflow executes multiple replicas of a high-variance operator in parallel and selects the result of the replica that finishes first. Here, we construct a 3-stage pipeline; the first and third operators do no computation. The second function draws a sample from one of three Gamma distributions and sleeps for the amount of time returned by the sample. For each Gamma distribution the shape parameter is  $k = 3$  and the scale parameter is  $\theta \in \{1, 2, 4\}$  corresponding to low, medium, and high variances.

We expect that increasing the number of replicas, particularly for high variance distributions, will noticeably reduce tail latencies. Figure 5 shows our results—the boxes show the interquartile range, and the whiskers show the 1st and 99th percentiles. In all cases, increasing from 1 to 3 replicas reduces *all* latencies significantly: tail latencies decreased

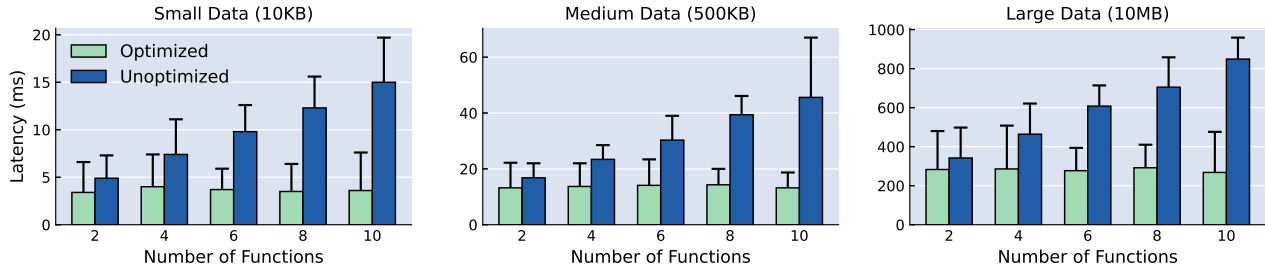


Figure 4: Median (bar) and 99th percentile (whisker) latencies for functions chains (length 2 to 10) with varying data sizes (10KB to 10MB).

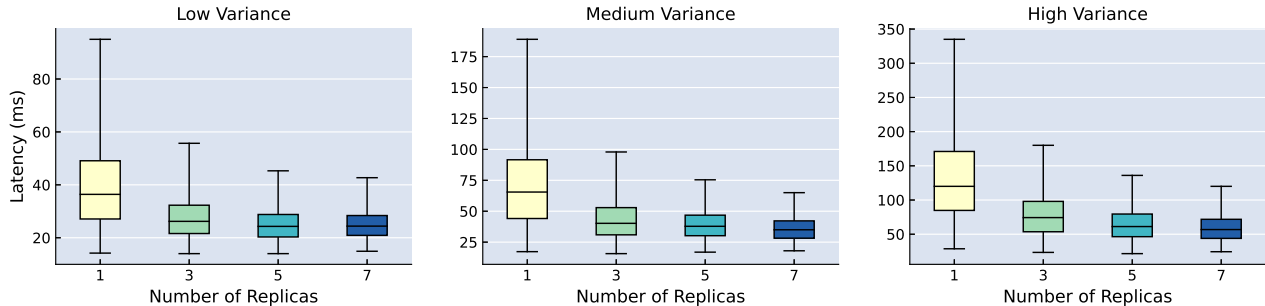


Figure 5: Latencies (1st, 25th, 50th, 75th, and 99th percentile) as a function of the number of additional replicas computed of a high-variance function.

71%, 94%, and 86% for low, medium, and high variances, and median latencies decreased 39%, 63%, and 62%.

Beyond 3 replicas, higher variance models see larger improvements. For the low variance dataflow, increasing from 3 to 7 replicas yields a 30% improvement in tail latency and only a 7% improvement at median. However, for the high variance setting, we observe a 50% improvement at the tail and a 31% improvement in median latency.

**Takeaway:** *Increasing the number of replicas reduces both tail and median latencies, with particularly significant improvements for extremely highly-variable dataflows.*

### 5.1.3 Operator Autoscaling

In this section, we look at Cloudflow’s and Cloudburst’s ability to respond to load changes with fine-grained operator scaling. We study a workload with two functions—one fast and one slow—similar to the example from Section 4. We introduce a sudden load spike and measure latency, throughput, and resource allocation. Figure 6 shows our results. We begin with 4 client threads issuing requests simultaneously; latency and throughput are steady. There are 3 threads allocated to the slow function and 1 thread allocated to the fast function.

At 15 seconds, we introduce a 4× load spike. Latency immediately increases as the allocated resources are saturated. The autoscaler responds by adding 16 replicas of the slow function over 15 seconds, and after time 40, latency returns to pre-spike levels (with a minor blip); throughput stabilizes at a new high. In the meantime, there is no change in the resource allocation of the fast function—it remains at 1 replica.

Over the remaining minute, the autoscaler adds 2 more replicas of the slow function to introduce slack into the system. This is because the existing resource allocation matches the incoming request rate exactly, and the autoscaler creates a small amount of excess capacity to account for potential future load spikes. There is no increase in throughput because the existing resources were sufficient to service the incoming request rate. This type of fine-grained resource allocation is especially useful for pipelines with heterogeneous resource requirements—a user would not want to scale up GPU allocation beyond necessary for a pipeline is bottlenecked on a CPU task.

**Takeaway:** *Cloudflow’s dataflow model allows for fine-grained resource allocation in the underlying serverless runtime, enabling nimble responses to load changes while ensuring efficient use of resources.*

### 5.1.4 Locality

Next, we look at the benefits of data locality. We picked a representative task in which we access each of a small set of objects (100) a few times (10) in a random order. The pipeline consists of a map that pick which object to access, a lookup of the object, and a second map that computes a result (the sum of elements in an array). We vary the size of the retrieved data from 8KB to 8MB. Figure 7 shows our results. In all settings, we warm up the Cloudburst’s caches by issuing a request for each data item once before starting the benchmark.

As described in Section 4, Cloudflow’s locality optimization has two components: (1) fusing lookups with downstream operators and (2) enabling dynamic dispatch to take

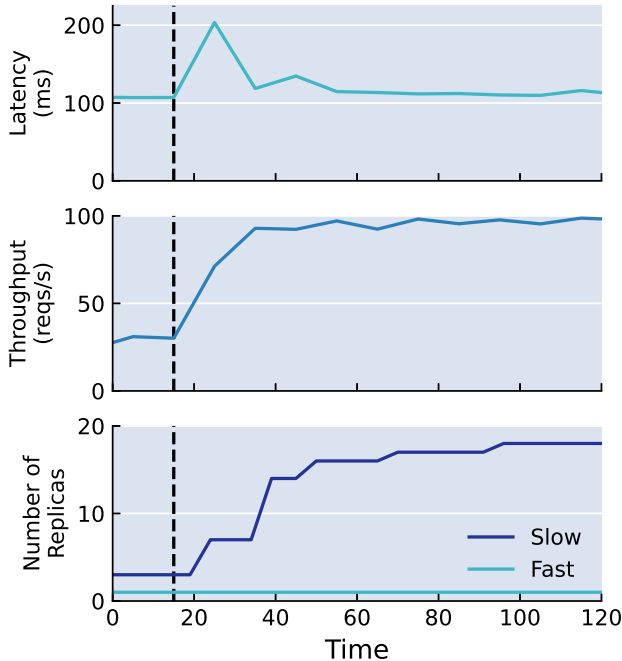


Figure 6: Median latency, throughput, and resource allocation in response to a load spike for a pipeline with a fast and a slow function.

advantage of Cloudburst’s scheduling heuristics. We measure the incremental benefits of both these rewrites. The Naive bar Figure 7 implements neither optimization—data is retrieved from the KVS in the execution of the `lookup` operator and shipped downstream to the next operator. The Fusion Only bar merges the `lookup` with the second `map` but does not use dynamic dispatch. The Fusion + Dispatch bar uses both optimizations.

For small data sizes, our optimizations make little difference—the cost of shipping 8KB of data is low, and the Naive implementation is only 2.5ms slower than having both optimizations implemented. As we increase data size, however, Naive performance significantly worsens—for each

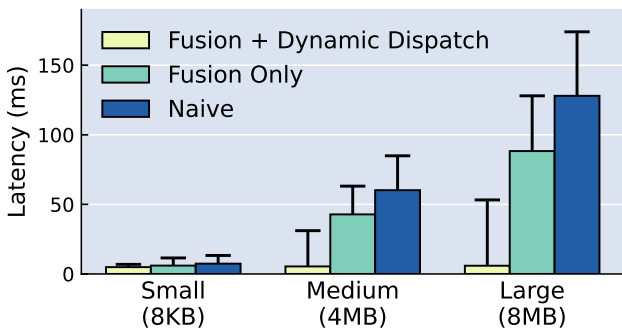


Figure 7: Median latency and 99th percentile latencies for a data-intensive pipeline on Cloudflow with the fusion and dynamic dispatch optimizations enabled, only fusion enabled, and neither enabled.

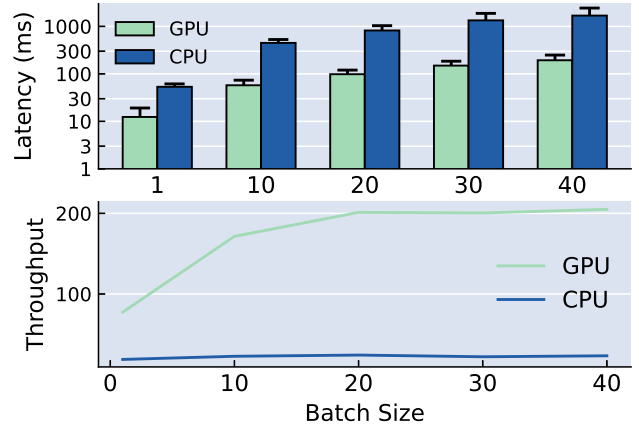


Figure 8: A comparison of CPUs and GPUs on Cloudflow, measuring latency and throughput while varying the batch size for the ResNet-101 computer vision model.

request, data is moved once from the KVS to the `lookup` operator and again from the `lookup` to the second `map`. The Fusion Only operator avoids *one* hop of data movement (between operators), but relies on random chance to run on a machine where its input data is cached—this does not happen very often. With the dynamic dispatch optimization implemented, Cloudflow takes advantage of locality-aware scheduling and for the largest data size (8MB) is  $15\times$  faster than Fusion Only and  $22\times$  faster than Naive. Tail latencies, however, do increase noticeably with data size, as the requests that incur cache misses will still pay data shipping costs.

**Takeaway:** Cloudflow’s locality optimizations enable it to avoid data shipping costs and lead to an order of magnitude improvement in latencies for non-trivial data accesses.

### 5.1.5 Batching

Finally, we look at the benefits of batching. In this experiment, we introduce GPUs, since batching primarily benefits with highly parallel hardware. We execute a pipeline with a single model (the ResNet-50 [22] image classification model in PyTorch) and no other operators. Enabling batching required changing only two lines of user code—using `torch.stack` to combine inputs into a single tensor. Our experiment varies the batch size from 1 to 40 in increments of 10. We asynchronously issue  $k$  requests (where  $k$  is the batch size) from a single client in order to control the batch size and measure the time until all results are returned. Figure 8 reports latency (on a log-scale) and throughput for each batch size.

At baseline (batch size 1), the GPU has a roughly  $4\times$  better latency and throughput than the CPU. Increasing the batch size for the CPU from 1 to 10 yields a 20% increase in throughput (18 to 22 requests) with an  $8\times$  increase in latency. Beyond that point, latency increases linearly and throughput plateaus—standard CPUs do not support parallel execution.

On a GPU, we see a  $4.5\times$  jump in latency and  $2.2\times$  increase in throughput from size 1 to 10. Between 10 and 20, we see a further 70% increase in latency with only an 18% increase in throughput. Past size 20, the GPU is saturated; throughput plateaus and latency increases linearly with batch size. Note that between batch sizes 1 and 20, there is only an  $8\times$  increase in latency (12ms to 100ms)—well within the bounds for an interactive web application [23]—while significantly improving the throughput ( $3\times$ ).

**Takeaway:** *Cloudflow's batching optimization enables a  $3\times$  increase in throughput while retaining interactive latency.*

## 5.2 Prediction Serving Pipelines

Having measured Cloudflow in isolation, we now look at real prediction serving pipelines and compare Cloudflow to state-of-the-art commercial and research systems: AWS Sagemaker and Clipper [10]. AWS Sagemaker is a hosted, end-to-end platform for managing machine learning models that includes a containerized deployment tool. We selected it as a representative of a number of hosted model management tools with prediction serving capabilities. Clipper is an open-source research platform that automatically containerizes and deploys models while maintaining strict latency goals. We measure Cloudflow against both systems on four real world pipelines: an image cascade, a video processing pipeline, a neural machine translation task, and a recommender system.

For each pipeline, we sampled multiple optimization strategies on Cloudflow. Due to space limits, we do not describe results from each configuration; we limit ourselves to the optimization strategies that worked best and the corresponding results. We return to automating the optimization process in Section 7.

### 5.2.1 Pipelines

**Image Cascade.** A cascade pipeline (described in Section 3.2) chains together models of increasing complexity, executing later models only if the earlier models are unsure of their predictions. We use a cascade with two models: ResNet-101 [22] and Inception v3 [54]. We preprocess an input image

```

1 flow = cloudflow.Dataflow([('img', numpy.ndarray)])
2 img = flow.map(preprocess)
3 resnet = img.map(resnet_101)
4 inception = resnet.filter(low_confidence).map(inception_v3)
5 label = resnet.join(inception).map(pick_best_prediction)
6
7 category_counts = people.union(vehicles).groupby('category')
8     .agg('count')
9 label = category_counts
10 flow.output = label

```

Figure 9: The Cloudflow implementation of the image cascade pipeline in Section 5.2.

and execute ResNet; if ResNet's confidence is below 85%, we then execute Inception and pick the result with the higher confidence. We run this pipeline with a random sample of images from the ImageNet dataset [48].

**Video Streams.** Processing video streams is an extremely data- and compute-intensive task. We use a standard video processing flow [62] that uses YOLOv3 [47] to classify the frames of a short video clip (1 second). Based on the YOLO classifications, we select frames that contain people and vehicles (representative of a pipeline for an autonomous vehicle) and send those frames to one of two ResNet-101 models. The two ResNet models are executed in parallel and more specifically classify people and vehicles, respectively. We union the results of the two models, group by the ResNet classifications, and count the occurrences of each class per input clip.

**Neural Machine Translation.** Models that translate text between languages are becoming increasingly widely used (e.g., chat applications, social networks). These models are also notoriously large and computationally intensive. We model a translation task by first classifying an input text's language using fastText, an open-source language modeling library [29, 30]. We limit our inputs to French and German. Based on the language classification, we then feed a second input into one of two models that translates between English and the classified language. The translation models are implemented in the PyTorch FAIRSEQ library [45] based on sequence learning translation models [17].

**Recommender System.** Recommender systems are ubiquitous among internet services. Facebook recently published a case study of their DNN-based personalized recommenders [19]; we implement a pipeline modeled after their architecture. A request comes in with a user ID and recent items the user has clicked on; based on the set of recently clicked items, we generate a product category recommendation. The pipeline then computes a top- $k$  set of items from that product category, using the user's pre-calculated weight vector. This is done with a simple matrix multiplication-based scoring scheme. While the user vectors are small (length 512), the product category sets can be large (roughly 10MB)—as a result, enabling locality and minimizing data movement is an important part of implementing these pipelines efficiently.

```

1 flow = cloudflow.Dataflow([('frame', numpy.ndarray)])
2 yolo_preds = flow.map(yolov3)
3 people = yolo_preds.map(resnet101_people)
4 vehicle = yolo_preds.map(resnet101_vehicles)
5 category_counts = people.union(vehicles).groupby('category')
6     .agg('count')
7 label = category_counts
8 flow.output = label

```

Figure 10: The Cloudflow implementation of the video stream processing pipeline in Section 5.2.

### 5.2.2 Benchmark Setup

**Cloudflow.** For each pipeline, we start with one replica per operator and run a 200 request warm-up phase that allows the Cloudburst autoscaler to settle on a resource allocation. We then run 1,000 requests from 10 benchmark clients in parallel and report median latency, 99th percentile latency, and throughput below. Unless stated otherwise, we copied the exact resource allocation from Cloudflow to each of the other systems.

**Sagemaker.** Sagemaker requires users to provide a Docker container per pipeline stage—a cumbersome and time-consuming process. We wrap each pipeline stage in a bespoke container and deploy it as a Sagemaker endpoint. We do not rely on Sagemaker’s built-in inference pipelines feature, as it does not support parallelism, which is required in our workloads. Instead, we built a proxy service that manages each client request as it passes through the pipeline. This enables us to invoke multiple endpoints in parallel when necessary. CPU workers in Sagemaker used `m1.c5.2xlarge` instances, and GPU workers used `m1.g4dn.xlarge` instances.

**Clipper.** Clipper is a state-of-the-art research system that, similar to Sagemaker, deploys models as microservices; Clipper does not support pipelines in any form. Similar to our Sagemaker deployments, we use custom code to move each request through the pipeline. Deploying models using Clipper’s API was easier than with Sagemaker, but certain pipelines with bespoke dependencies required us to build custom Docker containers. The simplest way to deploy model replicas on Clipper was to create multiple replicas of the model on a large machine—however, we ensured that the number of resources (vCPUs, RAM, and GPUs) per worker was the same as on Cloudflow and Sagemaker. Note that Clipper also supports batching, which we enabled for GPU workloads.

### 5.2.3 Results

We report results for each pipeline in Section 5.2.1 on both CPU and GPU deployments, except for the recommender system, which we only run on CPU. We omit GPU results for this pipeline because, as noted by [19], recommendation models have low arithmetic intensity and do not usually benefit

```
1 flow = cloudflow.Dataflow([('english', str), ('other', str)
2                               ])
3 language_type = flow.map(yolov3)
4 french = language_type.filter(is_french).map(
5     translate_from_french)
6 german = language_type.filter(is_german).map(
7     translate_from_german)
8 result = german.join(french)
9 flow.output = result
```

Figure 11: The Cloudflow implementation of the neural machine translation pipeline in Section 5.2.

from GPU acceleration. Unless stated otherwise, we enabled batching on Cloudflow and Clipper for all GPU workloads and disabled it for all CPU workloads, as per our results in Section 5.1.5.

**Image Cascade.** The leftmost graph in Figure 13 shows results for the image cascade. We enabled Cloudflow’s fusion optimization and merged the whole pipeline into a single operator. Despite having a mix of CPU and GPU operators in the pipeline, we found that the CPU execution costs were low (10-15ms) and that reducing data movement best improved Cloudflow’s performance.

On both CPU and GPU deployments, Cloudflow has a roughly  $2\times$  better median latency than the other systems. This translates into a  $2\times$  increase in throughput for both hardware configurations. These improvements are largely due to reduced data movement costs enabled by operator fusion. We also note the benefits of batching by comparing Clipper and Sagemaker’s performance. In CPU mode where neither system uses batching, Sagemaker outperforms Clipper by 20%; however, in GPU mode, where Clipper supports batching and Sagemaker does not, Clipper is able to close the performance gap and *match* Sagemaker’s throughput.

**Video Streams.** The video streaming pipeline was the most data intensive: Each video input had 30 frames, which was about 20MB of data. In this pipeline, there were only GPU models (YOLOv3 and ResNet-101) without any CPU stages—we again apply operator fusion to the whole pipeline to generate a single Cloudburst function. We found that the cost of executing the two parallel ResNet instances in serial was lower than the cost of shipping the input over the network.

CPU deployments are expectedly slow—Cloudflow’s median latency was 3.1 seconds, while Sagemaker’s and Clipper’s were around 4.4 seconds; tail latencies were 4.4, 6.7, and 7.9 seconds respectively. Cloudflow’s reduced data movement enables significant improvements (41% at median and up to 80% at the 99th percentile) but was still capped at 3.1 requests per second.

Results are much more promising for GPU deployments. Cloudflow’s median latency was 685ms, and its 99th percentile latency was about 1 second (996ms)—meaning that Cloudflow can consistently process video in real-time. Sagemaker and Clipper were both slower, with median latencies

```
1 flow = cloudflow.Dataflow([('uid', int), ('recent_clicks',
2                               numpy.ndarray)])
3 topk_for_user = flow.lookup('uid', type='column_ref') \
4     .map(pick_category) \
5     .lookup('category', type='column_ref')
6     .map(get_topk)
7 flow.output = topk_for_user
```

Figure 12: The Cloudflow implementation of the recommender system pipeline in Section 5.2.

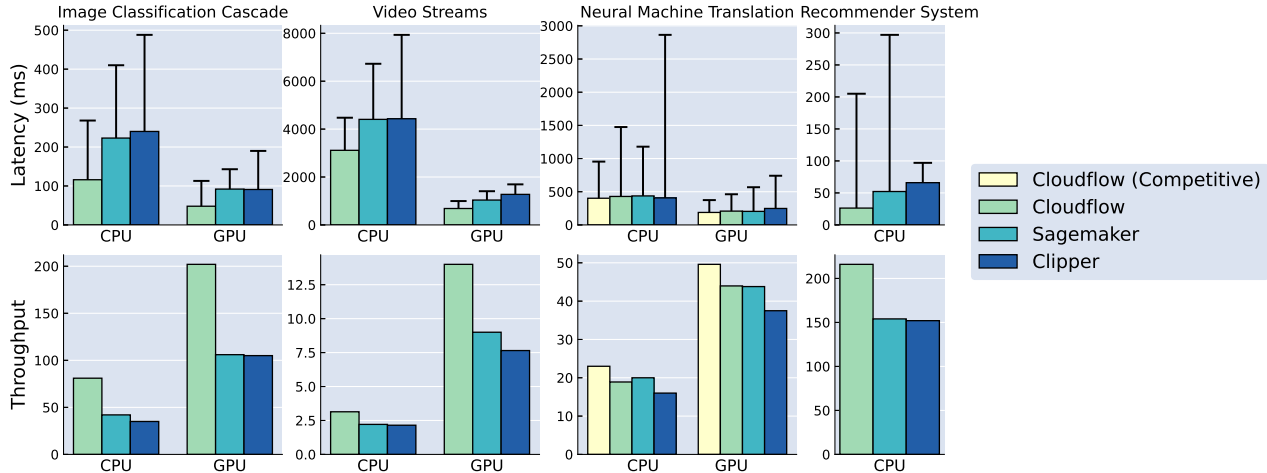


Figure 13: Latencies and throughputs for each of the four pipelines described in Section 5.2.1 on Cloudflow, AWS Sagemaker, and Clipper.

of 1 and 1.3 seconds, respectively, and 99th percentile latencies at 1.4 and 1.7s seconds. Cloudflow is able to process 14 requests per second, while the other systems were both below 9 requests a second.

**Neural Machine Translation.** The neural machine translation task was the best case scenario for both Clipper and Sagemaker as it had the least input data (strings to translate) while being very computationally intensive. We found that the NMT models—particularly on CPU—had high variance in runtimes, so we enabled competitive execution in Cloudflow. However, since competitive execution required allocating extra resources not available to Sagemaker and Clipper, we report Cloudflow measurements with and without competitive execution.

On CPUs, the median latencies for all configurations are similar—Clipper was about 7% faster than Sagemaker and Cloudflow without competition. At the tail, Clipper was the slowest with a 99th percentile of 2.8 seconds; Cloudflow’s tail latency was 1.5 seconds, and Sagemaker’s was 1.2 seconds. Despite a 25% lower tail latency, Sagemaker’s throughput was only 5% higher than Cloudflow’s. Adding two competitive replicas reduced Cloudflow’s median latency by 7% and its 99th percentile by over 50%. This led to a 20% improvement in throughput compared to Cloudflow without competition and 15% improvement over Sagemaker.

On the GPU deployment, Cloudflow without competition and Sagemaker had similar performance. Clipper’s median latency was about 20% higher, likely because its scheduler constructs batches more aggressively than Cloudflow does. Cloudflow without competition and Sagemaker had the same throughput, while Clipper’s was 15% lower. Introducing competitive GPU replicas lowered median latencies by 10% and lowered tail latency by almost 25% relative to Cloudflow without competition (and by over 50% relative to Sagemaker). This translated into a 13% improvement in throughput.

**Recommender System.** Finally, we look at the recommender

pipeline. This workload was different from the others because it was data-intensive and computationally light—each request required only a matrix multiplication followed by a few simple operations. The user weight vectors and product categories in this pipeline are pre-generated. That provides an opportunity for us to exercise Cloudflow’s locality aware scheduling.

Running on Cloudburst allows us to automatically access data in Anna; however, Sagemaker blocks inbound network connections, which Anna requires, as it is an asynchronous KVS. As a workaround we used AWS ElastiCache’s hosted Redis offering, which has similar performance to Anna [58], as the storage engine for Clipper and Sagemaker. To simulate the caches in Cloudburst, we also added in-memory caches of size 2GB to Sagemaker and Clipper, that allowed them to cache user weight vectors and product categories—however, these systems do not have Cloudflow’s dynamic dispatch, so the likelihood of a cache miss is much higher. We pre-generate 100,000 user weight vectors (length 512, 4KB each) and 1,000 product categories (2,500 products per category, 10MB each) and put them in storage. For each request, we input a random user ID and a random set of recent clicks—this translates to a random product category per request.

Cloudflow’s locality optimizations lead to a  $2\times$  improvement in median latency over Sagemaker’s and  $2.5\times$  improvement over Clipper’s. Cloudflow reliably places requests on machines with cached inputs, whereas Sagemaker and Clipper are much less likely to see cache hits. Tail latencies for all systems are high due to the cost of retrieving data over the network. Nonetheless, the lower median latencies translate to a roughly 40% increase in throughput over Sagemaker and Clipper.

**Takeaway:** Cloudflow’s optimizations enable it to outperform state-of-the-art prediction serving systems up to  $2\times$  on real-world tasks; importantly, it is able to meet real-time latency goals for a data- and compute-intensive task like video streaming.

## 6 Related Work

**Dataflow Abstractions.** Dataflow abstractions have deep roots in both software and hardware architectures (e.g., [12, 13]). In the last decade, dataflow emerged as a core programming abstraction for systems such as Spark [61] and Dryad [26] that excel in high throughput big data processing. Other systems like Naiad [44], Flink [8], and Noria [18, 49] implement stateful dataflow that targets scenarios where the input data continuously streams into the system. Cloudflow, in comparison, is designed for handling interactive model serving queries at low latency, and the input of each query is bounded. In addition to standard dataflow optimizations such as operator fusion, Cloudflow implements a variety of custom optimizations that are well-suited to interactive model serving, such as competitive execution and fine-grained autoscaling.

**Packet Processing and Distributed Systems.** Programmable packet processors for networks share our latency focus, but target much less compute-intensive tasks than model serving, using lower-level optimizations. The Click router [34] is an influential example; subsequent work in declarative networking [40] and packet processing languages [6] provide higher-level abstractions that often compile down to dataflow. Similar languages have targeted distributed systems [2, 41, 43], with a focus on orthogonal concerns like coordination avoidance.

**Lightweight Event Flows.** Systems such as SEDA [57] adapt the resource allocation of different stages of a pipeline based on demand, but do not have a semantic notion of the tasks’ meanings and thus cannot perform logical rewrites of the pipeline. Additionally, SEDA is focused on single-server rather than distributed executions and has no autoscaling.

**ML Optimizations.** TASO [27] and ParM [36] introduce optimizations on individual models that can be integrated into prediction serving systems. TASO performs low-level rewrites of DNN computation graphs to improve model performance. ParM reduces the tail latencies and enables failure recovery for variable models by using erasure coding to reconstruct slow and failed predictions. Neither system offers end-to-end optimizations similar to Cloudflow’s.

**Prediction Serving Systems.** Clipper [10], TFServe [4], Azure ML [55], and AWS Sagemaker either have no support for pipelines or impose restrictions on the topology of the pipelines. As such, none of these systems perform pipeline optimizations as in Cloudflow. Other systems such as Inferline [9] and Pretzel [37] are complementary to Cloudflow; Inferline focuses on efficient scheduling to meet latency goals, and Pretzel exploits white-box pipelines to optimize individual stages. We plan to explore both of these approaches in future work.

## 7 Conclusion and Future Work

In this paper, we presented Cloudflow, a dataflow framework for prediction serving pipelines. Cloudflow offers a familiar dataflow programming API that allows developers to easily construct prediction pipelines in a few lines of code. We transparently implement two kinds of optimizations over the resulting dataflow graph: dataflow rewrites and dataflow-to-FaaS compilation. Cloudflow deploys pipelines on top of Cloudburst, a low-latency, stateful Function-as-a-Service platform; we extended Cloudburst with key features to support our workloads.

Our evaluation shows that Cloudflow’s automated optimizations enable us to outperform state-of-the-art prediction serving systems by up to  $2\times$  for real-world tasks like image cascades and video processing. Our architecture and optimization scheme suggest a number of interesting avenues for future work.

**Automated Optimization Selection.** Currently, we require manual selection of optimizations best-suited to each workload. There is a rich history of automated optimization of programs—including dataflows—in the database, systems and programming languages literature. Techniques like cost-based database query optimization would seem to be a good fit to our API, but will require research to address our heterogeneous operators, hardware, and latency goals.

**Meeting Latency SLAs.** We have focused in this work on reducing latency, but we have not thus far considered techniques for managing Service Level Agreements (SLAs) or Objectives (SLOs) regarding latency deadlines. Having explicit deadlines—with cost penalties for missing them—brings multi-objective tradeoffs into the picture, which makes the optimization problems we consider more complex.

**Verifying Dataflow Correctness.** As we alluded to in Section 3.1, Cloudflow provides runtime type checking of dataflows. However, there are other changes in machine learning pipelines—e.g., a video monitoring camera inadvertently is turned to face a wall—that can lead to failures without type errors. TFX [4] helps detect these issues by capturing statistics about the inputs to its models; we plan to bring such capabilities into the existing type monitoring in Cloudflow. We also plan to extend the debuggability of Cloudflow by adding anomaly detection over the passively captured statistics about inputs and outputs.

## References

- [1] M. Abadi, P. Barham, J. Chen, Z. Chen, A. Davis, J. Dean, M. Devin, S. Ghemawat, G. Irving, M. Isard, et al. Tensorflow: A system for large-scale machine learning. In *12th {USENIX} Symposium on Operating Systems Design and Implementation ({OSDI} 16)*, pages 265–283, 2016.

- [2] P. Alvaro, N. Conway, J. M. Hellerstein, and W. R. Marczak. Consistency analysis in bloom: a calm and collected approach. In *CIDR*, pages 249–260, 2011.
- [3] G. Antoshenkov. Dynamic query optimization in rd-b/vms. In *Proceedings of IEEE 9th International Conference on Data Engineering*, pages 538–547. IEEE, 1993.
- [4] D. Baylor, E. Breck, H.-T. Cheng, N. Fiedel, C. Y. Foo, Z. Haque, S. Haykal, M. Ispir, V. Jain, L. Koc, et al. Tfx: A tensorflow-based production-scale machine learning platform. In *Proceedings of the 23rd ACM SIGKDD International Conference on Knowledge Discovery and Data Mining*, pages 1387–1395, 2017.
- [5] S. Bianco, R. Cadene, L. Celona, and P. Napoletano. Benchmark analysis of representative deep neural network architectures. *IEEE Access*, 6:64270–64277, 2018.
- [6] P. Bosshart, D. Daly, G. Gibb, M. Izzard, N. McKeown, J. Rexford, C. Schlesinger, D. Talayco, A. Vahdat, G. Varghese, et al. P4: Programming protocol-independent packet processors. *ACM SIGCOMM Computer Communication Review*, 44(3):87–95, 2014.
- [7] S. Breß and G. Saake. Why it is time for a hype: A hybrid query processing engine for efficient gpu coprocessing in dbms. *Proceedings of the VLDB Endowment*, 6(12):1398–1403, 2013.
- [8] P. Carbone, A. Katsifodimos, S. Ewen, V. Markl, S. Haridi, and K. Tzoumas. Apache flink: Stream and batch processing in a single engine. *Bulletin of the IEEE Computer Society Technical Committee on Data Engineering*, 36(4), 2015.
- [9] D. Crankshaw, G. Sela, C. Zumar, X. Mo, J. E. Gonzalez, I. Stoica, and A. Tumanov. Inferline: ML inference pipeline composition framework. *CoRR*, abs/1812.01776, 2018.
- [10] D. Crankshaw, X. Wang, G. Zhou, M. J. Franklin, J. E. Gonzalez, and I. Stoica. Clipper: A low-latency online prediction serving system. In *14th {USENIX} Symposium on Networked Systems Design and Implementation ({NSDI} 17)*, pages 613–627, 2017.
- [11] J. Dean and S. Ghemawat. Mapreduce: simplified data processing on large clusters. *Communications of the ACM*, 51(1):107–113, 2008.
- [12] J. B. Dennis. First version of a data flow procedure language. In *Programming Symposium*, pages 362–376. Springer, 1974.
- [13] J. B. Dennis and D. P. Misunas. A preliminary architecture for a basic data-flow processor. In *Proceedings of the 2nd annual symposium on Computer architecture*, pages 126–132, 1974.
- [14] T. Z. J. Fu, J. Ding, R. T. B. Ma, M. Winslett, Y. Yang, and Z. Zhang. Drs: Auto-scaling for real-time stream analytics. *IEEE/ACM Trans. Netw.*, 25(6):3338–3352, Dec. 2017.
- [15] A. Gandhi, M. Harchol-Balter, R. Raghunathan, and M. A. Kozuch. Autoscale: Dynamic, robust capacity management for multi-tier data centers. *ACM Trans. Comput. Syst.*, 30(4):14:1–14:26, Nov. 2012.
- [16] P. Gao, L. Yu, Y. Wu, and J. Li. Low latency rnn inference with cellular batching. In *Proceedings of the Thirteenth EuroSys Conference*, pages 1–15, 2018.
- [17] J. Gehring, M. Auli, D. Grangier, D. Yarats, and Y. N. Dauphin. Convolutional sequence to sequence learning. *CoRR*, abs/1705.03122, 2017.
- [18] J. Gjengset, M. Schwarzkopf, J. Behrens, L. T. Araújo, M. Ek, E. Kohler, M. F. Kaashoek, and R. Morris. Noria: dynamic, partially-stateful data-flow for high-performance web applications. In *13th USENIX Symposium on Operating Systems Design and Implementation (OSDI 18)*, pages 213–231, Carlsbad, CA, Oct. 2018. USENIX Association.
- [19] U. Gupta, C.-J. Wu, X. Wang, M. Naumov, B. Reagen, D. Brooks, B. Cottel, K. Hazelwood, M. Hempstead, B. Jia, et al. The architectural implications of facebook’s dnn-based personalized recommendation. In *2020 IEEE International Symposium on High Performance Computer Architecture (HPCA)*, pages 488–501. IEEE, 2020.
- [20] K. Hazelwood, S. Bird, D. Brooks, S. Chintala, U. Diril, D. Dzhulgakov, M. Fawzy, B. Jia, Y. Jia, A. Kalro, et al. Applied machine learning at facebook: A datacenter infrastructure perspective. In *2018 IEEE International Symposium on High Performance Computer Architecture (HPCA)*, pages 620–629. IEEE, 2018.
- [21] K. Hazelwood, S. Bird, D. Brooks, S. Chintala, U. Diril, D. Dzhulgakov, M. Fawzy, B. Jia, Y. Jia, A. Kalro, J. Law, K. Lee, J. Lu, P. Noordhuis, M. Smelyanskiy, L. Xiong, and X. Wang. Applied machine learning at facebook: A datacenter infrastructure perspective. In *2018 IEEE International Symposium on High Performance Computer Architecture (HPCA)*, pages 620–629, Feb 2018.
- [22] K. He, X. Zhang, S. Ren, and J. Sun. Deep residual learning for image recognition. In *Proceedings of the IEEE conference on computer vision and pattern recognition*, pages 770–778, 2016.

- [23] Y. He, S. Elnikety, J. Larus, and C. Yan. Zeta: Scheduling interactive services with partial execution. In *Proceedings of the Third ACM Symposium on Cloud Computing*, pages 1–14, 2012.
- [24] J. M. Hellerstein, J. Faleiro, J. E. Gonzalez, J. Schleier-Smith, V. Sreekanti, A. Tumanov, and C. Wu. Serverless computing: One step forward, two steps back. *arXiv preprint arXiv:1812.03651*, 2018.
- [25] S. Hendrickson, S. Sturdevant, T. Harter, V. Venkataramani, A. C. Arpaci-Dusseau, and R. H. Arpaci-Dusseau. Serverless computation with openlambda. In *8th {USENIX} Workshop on Hot Topics in Cloud Computing (HotCloud 16)*, 2016.
- [26] M. Isard, M. Budiu, Y. Yu, A. Birrell, and D. Fetterly. Dryad: Distributed data-parallel programs from sequential building blocks. In *Proceedings of the 2nd ACM SIGOPS/EuroSys European Conference on Computer Systems 2007, EuroSys '07*, page 59–72, New York, NY, USA, 2007. Association for Computing Machinery.
- [27] Z. Jia, O. Padon, J. Thomas, T. Warszawski, M. Zaharia, and A. Aiken. Taso: Optimizing deep learning computation with automatic generation of graph substitutions. In *Proceedings of the 27th ACM Symposium on Operating Systems Principles, SOSP '19*, page 47–62, New York, NY, USA, 2019. Association for Computing Machinery.
- [28] M. Johnson, M. Schuster, Q. V. Le, M. Krikun, Y. Wu, Z. Chen, N. Thorat, F. Viégas, M. Wattenberg, G. Corrado, et al. Google’s multilingual neural machine translation system: Enabling zero-shot translation. *Transactions of the Association for Computational Linguistics*, 5:339–351, 2017.
- [29] A. Joulin, E. Grave, P. Bojanowski, M. Douze, H. Jégou, and T. Mikolov. Fasttext.zip: Compressing text classification models. *arXiv preprint arXiv:1612.03651*, 2016.
- [30] A. Joulin, E. Grave, P. Bojanowski, and T. Mikolov. Bag of tricks for efficient text classification. *arXiv preprint arXiv:1607.01759*, 2016.
- [31] N. P. Jouppi, C. Young, N. Patil, D. Patterson, G. Agrawal, R. Bajwa, S. Bates, S. Bhatia, N. Boden, A. Borchers, et al. In-datacenter performance analysis of a tensor processing unit. In *Proceedings of the 44th Annual International Symposium on Computer Architecture*, pages 1–12, 2017.
- [32] V. Kalavri, J. Liagouris, M. Hoffmann, D. Dimitrova, M. Forshaw, and T. Roscoe. Three steps is all you need: fast, accurate, automatic scaling decisions for distributed streaming dataflows. In *13th USENIX Symposium on Operating Systems Design and Implementation (OSDI 18)*, pages 783–798, Carlsbad, CA, Oct. 2018. USENIX Association.
- [33] V. Kalavri, J. Liagouris, M. Hoffmann, D. Dimitrova, M. Forshaw, and T. Roscoe. Three steps is all you need: Fast, accurate, automatic scaling decisions for distributed streaming dataflows. In *Proceedings of the 12th USENIX Conference on Operating Systems Design and Implementation, OSDI'18*, pages 783–798, Berkeley, CA, USA, 2018. USENIX Association.
- [34] E. Kohler, R. Morris, B. Chen, J. Jannotti, and M. F. Kaashoek. The click modular router. *ACM Transactions on Computer Systems (TOCS)*, 18(3):263–297, 2000.
- [35] J. Kosaian, K. Rashmi, and S. Venkataraman. Parity models: erasure-coded resilience for prediction serving systems. In *Proceedings of the 27th ACM Symposium on Operating Systems Principles*, pages 30–46, 2019.
- [36] J. Kosaian, K. V. Rashmi, and S. Venkataraman. Parity models: Erasure-coded resilience for prediction serving systems. In *Proceedings of the 27th ACM Symposium on Operating Systems Principles, SOSP '19*, page 30–46, New York, NY, USA, 2019. Association for Computing Machinery.
- [37] Y. Lee, A. Scolari, B.-G. Chun, M. D. Santambrogio, M. Weimer, and M. Interlandi. {PRETZEL}: Opening the black box of machine learning prediction serving systems. In *13th {USENIX} Symposium on Operating Systems Design and Implementation ({OSDI} 18)*, pages 611–626, 2018.
- [38] B. Lohrmann, P. Janacik, and O. Kao. Elastic stream processing with latency guarantees. In *2015 IEEE 35th International Conference on Distributed Computing Systems*, pages 399–410, June 2015.
- [39] B. Lohrmann, D. Warneke, and O. Kao. Nephelē streaming: Stream processing under qos constraints at scale. *Cluster Computing*, 17, 08 2013.
- [40] B. T. Loo, T. Condie, J. M. Hellerstein, P. Maniatis, T. Roscoe, and I. Stoica. Implementing declarative overlays. In *Proceedings of the Twentieth ACM Symposium on Operating Systems Principles, SOSP '05*, page 75–90, New York, NY, USA, 2005. Association for Computing Machinery.
- [41] C. Meiklejohn and P. Van Roy. Lasp: A language for distributed, coordination-free programming. In *Proceedings of the 17th International Symposium on Principles and Practice of Declarative Programming*, pages 184–195, 2015.

- [42] X. Meng, J. Bradley, B. Yavuz, E. Sparks, S. Venkataraman, D. Liu, J. Freeman, D. Tsai, M. Amde, S. Owen, et al. Mllib: Machine learning in apache spark. *The Journal of Machine Learning Research*, 17(1):1235–1241, 2016.
- [43] M. Milano, R. Recto, T. Magrino, and A. C. Myers. A tour of gallifrey, a language for geodistributed programming. In *3rd Summit on Advances in Programming Languages (SNAPL 2019)*. Schloss Dagstuhl-Leibniz-Zentrum fuer Informatik, 2019.
- [44] D. G. Murray, F. McSherry, R. Isaacs, M. Isard, P. Barham, and M. Abadi. Naiad: A timely dataflow system. In *Proceedings of the Twenty-Fourth ACM Symposium on Operating Systems Principles, SOSP '13*, page 439–455, New York, NY, USA, 2013. Association for Computing Machinery.
- [45] M. Ott, S. Edunov, A. Baevski, A. Fan, S. Gross, N. Ng, D. Grangier, and M. Auli. fairseq: A fast, extensible toolkit for sequence modeling. *CoRR*, abs/1904.01038, 2019.
- [46] A. Paszke, S. Gross, F. Massa, A. Lerer, J. Bradbury, G. Chanan, T. Killeen, Z. Lin, N. Gimelshein, L. Antiga, A. Desmaison, A. Kopf, E. Yang, Z. DeVito, M. Raison, A. Tejani, S. Chilamkurthy, B. Steiner, L. Fang, J. Bai, and S. Chintala. Pytorch: An imperative style, high-performance deep learning library. In H. Wallach, H. Larochelle, A. Beygelzimer, F. d'Alché-Buc, E. Fox, and R. Garnett, editors, *Advances in Neural Information Processing Systems 32*, pages 8024–8035. Curran Associates, Inc., 2019.
- [47] J. Redmon and A. Farhadi. Yolov3: An incremental improvement. *arXiv preprint arXiv:1804.02767*, 2018.
- [48] O. Russakovsky, J. Deng, H. Su, J. Krause, S. Satheesh, S. Ma, Z. Huang, A. Karpathy, A. Khosla, M. Bernstein, et al. Imagenet large scale visual recognition challenge. *International journal of computer vision*, 115(3):211–252, 2015.
- [49] M. Schwarzkopf. The remarkable utility of dataflow computing, 2020.
- [50] M. Shahradd, R. Fonseca, Í. Goiri, G. Chaudhry, P. Batum, J. Cooke, E. Laureano, C. Tresness, M. Russinovich, and R. Bianchini. Serverless in the wild: Characterizing and optimizing the serverless workload at a large cloud provider. *arXiv preprint arXiv:2003.03423*, 2020.
- [51] A. Singhvi, K. Houck, A. Balasubramanian, M. D. Shaikh, S. Venkataraman, and A. Akella. Archipelago: A scalable low-latency serverless platform. *arXiv preprint arXiv:1911.09849*, 2019.
- [52] V. Sreekanti, C. Wu, X. C. Lin, J. Schleier-Smith, J. M. Faleiro, J. E. Gonzalez, J. M. Hellerstein, and A. Tumanov. Cloudburst: Stateful functions-as-a-service, 2020.
- [53] L. Suresh, M. Canini, S. Schmid, and A. Feldmann. C3: Cutting tail latency in cloud data stores via adaptive replica selection. In *12th USENIX Symposium on Networked Systems Design and Implementation (NSDI 15)*, pages 513–527, Oakland, CA, May 2015. USENIX Association.
- [54] C. Szegedy, V. Vanhoucke, S. Ioffe, J. Shlens, and Z. Wojna. Rethinking the inception architecture for computer vision. *CoRR*, abs/1512.00567, 2015.
- [55] A. Team. Azureml: Anatomy of a machine learning service. In L. Dorard, M. D. Reid, and F. J. Martin, editors, *Proceedings of The 2nd International Conference on Predictive APIs and Apps*, volume 50 of *Proceedings of Machine Learning Research*, pages 1–13, Sydney, Australia, 06–07 Aug 2016. PMLR.
- [56] O. Trachsel and T. R. Gross. Variant-based competitive parallel execution of sequential programs. In *Proceedings of the 7th ACM International Conference on Computing Frontiers, CF '10*, page 197–206, New York, NY, USA, 2010. Association for Computing Machinery.
- [57] M. Welsh, D. Culler, and E. Brewer. Seda: an architecture for well-conditioned, scalable internet services. *ACM SIGOPS Operating Systems Review*, 35(5):230–243, 2001.
- [58] C. Wu, J. Faleiro, Y. Lin, and J. Hellerstein. Anna: A kvs for any scale. *IEEE Transactions on Knowledge and Data Engineering*, 2019.
- [59] C. Wu, V. Sreekanti, and J. M. Hellerstein. Autoscaling tiered cloud storage in anna. *Proceedings of the VLDB Endowment*, 12(6):624–638, 2019.
- [60] M. Zaharia, M. Chowdhury, T. Das, A. Dave, J. Ma, M. McCauly, M. J. Franklin, S. Shenker, and I. Stoica. Resilient distributed datasets: A fault-tolerant abstraction for in-memory cluster computing. In *Presented as part of the 9th {USENIX} Symposium on Networked Systems Design and Implementation ({NSDI} 12)*, pages 15–28, 2012.
- [61] M. Zaharia, R. S. Xin, P. Wendell, T. Das, M. Armbrust, A. Dave, X. Meng, J. Rosen, S. Venkataraman, M. J. Franklin, A. Ghodsi, J. Gonzalez, S. Shenker, and I. Stoica. Apache spark: A unified engine for big data processing. *Commun. ACM*, 59(11):56–65, Oct. 2016.

- [62] H. Zhang, G. Ananthanarayanan, P. Bodik, M. Philipose, P. Bahl, and M. J. Freedman. Live video analytics at scale with approximation and delay-tolerance. In *14th USENIX Symposium on Networked Systems Design and Implementation (NSDI 17)*, pages 377–392, Boston, MA, Mar. 2017. USENIX Association.
- [63] G. Zhou, X. Zhu, C. Song, Y. Fan, H. Zhu, X. Ma, Y. Yan, J. Jin, H. Li, and K. Gai. Deep interest network for click-through rate prediction. In *Proceedings of the 24th ACM SIGKDD International Conference on Knowledge Discovery & Data Mining*, pages 1059–1068, 2018.